

Enhanced photon-assisted spin transport in a quantum dot attached to ferromagnetic leads

Fabrício M. Souza, Thiago L. Carrara, and E. Vernek

Instituto de Física, Universidade Federal de Uberlândia, 38400-902, Uberlândia, MG, Brazil

(Date: January 19, 2019)

We investigate real-time dynamics of spin-polarized current in a quantum dot coupled to ferromagnetic leads in both parallel and antiparallel alignments. While an external bias voltage is taken constant in time, a gate terminal, capacitively coupled to the quantum dot, introduces a periodic modulation of the dot level. Using non equilibrium Green's function technique we find that spin polarized electrons can tunnel through the system via additional photon-assisted transmission channels. Owing to a Zeeman splitting of the dot level, it is possible to select a particular spin component to be photon-transferred from the left to the right terminal, with spin dependent current peaks arising at different gate frequencies. The ferromagnetic electrodes *enhance* or *suppress* the spin transport depending upon the leads magnetization alignment. The tunnel magnetoresistance also attains negative values due to a photon-assisted inversion of the spin-valve effect.

I. INTRODUCTION

Time-dependent transport in quantum dot system (QDs) has received significant attention due to a variety of new quantum physical phenomena emerging in transient time scale.¹ A few examples encompass charge pump^{2,3} and photon-assisted tunneling transport.⁴⁻⁸ For instance, in a double dot junction sandwiched by leads, if a sinusoidal gate voltage is applied among the dots, electrons can be pumped uphill from a lead with lower chemical potential to a lead with higher chemical potential, thus opposing to the usual dc-regime.⁹ Photon-assisted tunneling can occur when an oscillating gate potential or laser field is applied in a QD or a metallic central island coupled to source and drain terminals.⁴⁻¹⁰ Time-dependent regime also leads to zero-bias charge or spin pumping when a minimum set of two parameters of the system (e.g., gate potential and tunneling rate in a QD system) are time modulated independently. In particular, it was recently studied non-adiabatic charge and spin pumping through interacting quantum dots¹¹ and quantum transport pumping in graphene-based structures.¹²⁻¹⁵

Transient charge and spin dynamics in an interacting QD driven by step pulse or sinusoidal gate voltages revealed distinct charge and spin relaxation times.¹⁶ Based on time-dependent density functional theory and accounting for derivative discontinuity,¹⁷ it was also found that a current in a quantum dot system driven out-of-equilibrium by a fast switching on of the bias voltage develops self-sustained oscillations, due to dynamical Coulomb blockade,¹⁸ in contrast to the steady state expected behavior.

It is in the fascinating area of spintronics¹⁹ that time-dependent quantum transport reveals its prolific potentiality in producing spin polarized currents. For instance, a double dot structure driven by ac-field in the presence of magnetic field turn out to be a robust spin filtering and pumping device.^{20,21} By applying oscillating gates (radio frequency) in an open quantum dot in the presence of

Zeeman field, an adiabatic spin pump was generated.²²⁻²⁴ The current ringing¹ that arises in a quantum dot system when a bias voltage is suddenly switched on develops spin dependent beats when the dot level is Zeeman split.^{25,26} Coherent quantum beats in the current, spin current and tunnel magnetoresistance of two dots coupled to three ferromagnetic leads were also reported recently.²⁷ Additionally, spin spikes take place when a bias voltage is abruptly turned off in a system of a QD attached to ferromagnetic leads.^{28,29}

The study of quantum transport of spin polarized electrons in the presence of time varying fields was greatly motivated by the development of experimental techniques, that allows for the coherent control of the complete dynamics (initialization-manipulation-read out) of single electron spins in quantum dots.³⁰ Particularly, some of techniques used to coherently manipulate spin states are based on time dependent gate voltages.³¹⁻³⁶

In the present work we consider a single level quantum dot coupled to left and to right ferromagnetic leads in the presence of a static bias voltage and sinusoidal gate voltage. The oscillating gate potential introduces additional photon-assisted conduction channels, that can be tuned via a dc-gate field to lie within the conduction window of the system. In the presence of Zeeman splitting, produced by an applied magnetic field, the contribution from the photon-assisted channels becomes different for spins up and down, resulting in photon-assisted spin polarized currents. It is worth mentioning that this effect takes place even in the absence of ferromagnetic leads. However, when the leads are ferromagnetic and parallel aligned, the resonant current peaks are amplified for one spin component and suppressed for the other. Thus the photon-assisted current-polarization is enhanced. We also calculate the tunnel magnetoresistance (TMR) as a function of the gate frequency, which exhibits a variety of peaks and dips, having even a changed of sign, depending on the gate frequency.

The paper is organized as follows: in Sec.II we present the theoretical model and describe the formulation based on nonequilibrium Green's function technique and in

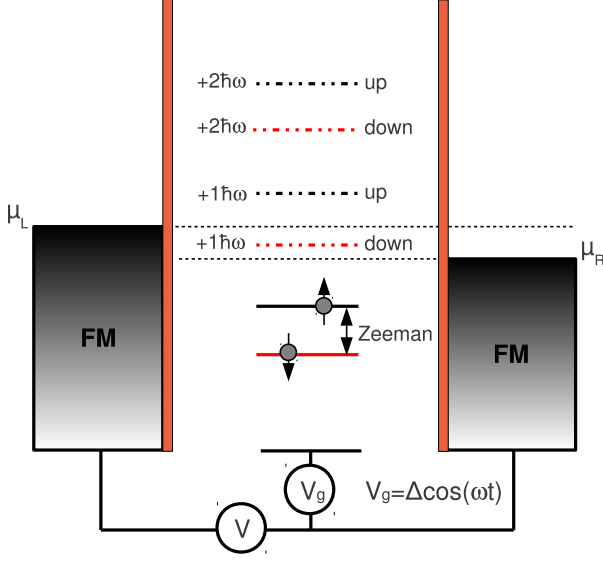


FIG. 1. Energy diagram for the system considered. A quantum dot is coupled to a left and to a right ferromagnetic electron reservoirs via tunneling barriers. The dot level is Zeeman split. A capacitively coupled gate terminal introduces a periodic perturbation of the dot level. This modulation induces additional photon-assisted channels (dashed lines) for spin polarized transport.

Sec. III we show and discuss the numerical results. Finally, in Sec. IV we present our concluding remarks.

II. MODEL AND THEORETICAL FORMULATION

For concreteness, the energy profile of our system is illustrated in Fig. 1 and is described by the Hamiltonian, $H = H_L + H_R + H_D(t) + H_T$, where

$$H_{L(R)} = \sum_{\mathbf{k}\sigma} \epsilon_{\mathbf{k}\sigma L(R)} c_{\mathbf{k}\sigma L(R)}^\dagger c_{\mathbf{k}\sigma L(R)}, \quad (1)$$

describes the free electrons in the (L) or the right (R) lead, in which $c_{\mathbf{k}\sigma L(R)}$ [$c_{\mathbf{k}\sigma L(R)}^\dagger$] is the operator that annihilates [creates] an electrons in the lead $L(R)$ with momentum \mathbf{k} , spin σ and energy $\epsilon_{\mathbf{k}\sigma L(R)}$. We consider a static source-drain applied voltage (V_{SD}) which drives the system out of equilibrium, breaking the left/right symmetry of the Hamiltonian. The time dependence of our Hamiltonian is fully accounted via the dot Hamiltonian,

$$H_D(t) = \sum_{\sigma} \epsilon_{\sigma}(t) d_{\sigma}^{\dagger} d_{\sigma}, \quad (2)$$

where $\epsilon_{\sigma}(t) = \epsilon_d(t) + \sigma E_Z/2$, with $\epsilon_d(t)$ being the time-dependent dot level and E_Z a Zeeman splitting of the dot

level due to an external magnetic field. Here we use $\sigma = +$ and $\sigma = -$ for spins up and down, respectively. The operator d_{σ} (d_{σ}^{\dagger}) annihilates (creates) one electron with spin σ and energy $\epsilon_{\sigma}(t)$ in the dot. In practice the time dependence in the dot level is controlled by an oscillating gate voltage $V_g(t)$, such that $\epsilon_d(t) = \epsilon^0 + V_g(t)$, where ϵ^0 is the dc component of the energy and $V_g(t) = \Delta \cos(\omega t)$ oscillates with amplitude Δ and frequency ω . Finally

$$H_T = \sum_{\mathbf{k}\sigma\eta} (V c_{\mathbf{k}\eta}^{\dagger} d_{\sigma} + V^* d_{\sigma}^{\dagger} c_{\mathbf{k}\sigma\eta}), \quad (3)$$

describes the tunnel coupling between the leads and the dot, with a constant coupling strength V and allows for current to flow across the QD.

To calculate the time dependent spin polarized current we employ the Keldysh Green's function formalism³⁷ that allows for an appropriate approach to our nonequilibrium time-dependent situation. Starting from the current definition $I_{\sigma}^{\eta}(t) = -e\langle \dot{N}_{\sigma} \rangle = -ie\langle [H, N_{\sigma}] \rangle$, where N_{σ} is the total number of particle operator for spin σ (here we take $\hbar = 1$), the current can be written as³⁸

$$I_{\sigma}^{\eta}(t) = 2e\text{Re}\left\{ \sum_k V G_{\sigma,k\sigma\eta}^{<}(t, t) \right\}, \quad (4)$$

where $G_{\sigma,k\sigma\eta}^{<}(t, t') = i\langle c_{k\sigma\eta}^{\dagger}(t') d_{\sigma}(t) \rangle$. Using the equation of motion technique and taking analytical continuation³⁷ to find $G_{\sigma,k\sigma\eta}^{<}(t, t')$ one finds to the current the following

$$I_{\sigma}^{\eta}(t) = -2e\Gamma_{\eta}^{\sigma} \text{Im}\left\{ \int \frac{d\epsilon}{2\pi} \int_{-\infty}^t dt_1 e^{-i\epsilon(t_1-t)} [G_{\sigma\sigma}^r(t, t_1) f_{\eta}(\epsilon) + G_{\sigma\sigma}^{<}(t, t_1)] \right\}, \quad (5)$$

where $f_{\eta}(\epsilon)$ is the Fermi distribution function of the η -th lead, and $\Gamma_{\sigma}^{\eta} = 2\pi|V|^2\rho_{\sigma}^{\eta}$ gives the tunneling rate between lead η and dot for spin component σ . ρ_{σ}^{η} is the density of states for spin σ in lead η . In the present model we assume constant density of states (wide-band limit). The ferromagnetism of the electrodes is modeled by considering $\Gamma_{\sigma}^{\eta} = \Gamma_0(1 \pm p_{\eta})$ where $+$ ($-$) stands for spin up (down), where p_{η} is the polarization of lead η -th^{39,40} and Γ_0 the tunneling rate strength.

Taking the time average of the current and assuming proportional coupling ($\Gamma_L^{\sigma} = \lambda \Gamma_R^{\sigma}$) we find

$$\langle I_{\sigma}^L(t) \rangle = -2e \frac{\Gamma_{\sigma}^L \Gamma_{\sigma}^R}{\Gamma_{\sigma}^L + \Gamma_{\sigma}^R} \int \frac{d\epsilon}{2\pi} [f_L(\epsilon) - f_R(\epsilon)] \text{Im}\langle A_{\sigma}(\epsilon, t) \rangle, \quad (6)$$

where

$$\langle A_{\sigma}(\epsilon, t) \rangle = \sum_{n=-\infty}^{\infty} J_n^2\left(\frac{\Delta}{\omega}\right) g_{n,\sigma}^R(\epsilon, \omega), \quad (7)$$

with $g_{n,\sigma}^R(\epsilon, \omega) = [\epsilon - \epsilon_{\sigma}^0 - n\omega + i\frac{\Gamma_{\sigma}^L + \Gamma_{\sigma}^R}{2}]^{-1}$. Here we used the fact that $\epsilon_{\sigma}(t) = \epsilon_{\sigma}^0 + \Delta \cos(\omega t)$, with $\epsilon_{\sigma}^0 = \epsilon^0 + \sigma E_Z/2$.

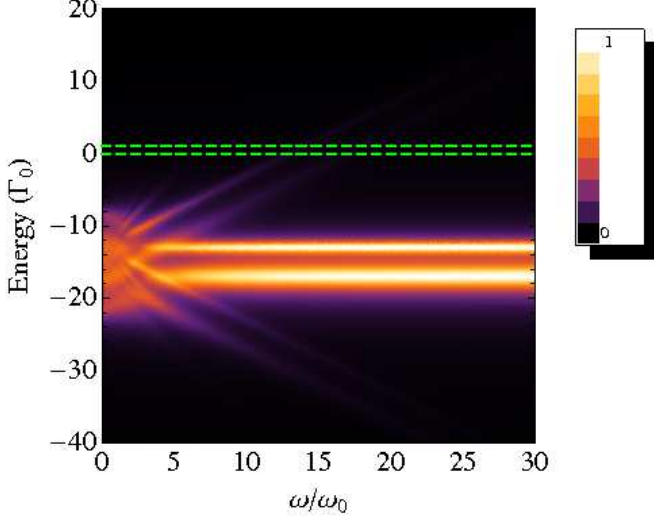


FIG. 2. Two dimensional map of the total transmission coefficient $T(\epsilon, \omega) = T_{\uparrow}(\epsilon, \omega) + T_{\downarrow}(\epsilon, \omega)$ as a function of frequency and energy in the parallel alignment ($p_L = p_R = -0.4$). For increasing ω , $T(\epsilon, \omega)$ develops additional photon-assisted peaks that allows off-resonant spin transport. The main two central peaks correspond to the Zeeman split levels $\epsilon_{\uparrow}^0 = \epsilon_0 + E_Z/2$ and $\epsilon_{\downarrow}^0 = \epsilon_0 - E_Z/2$. The satellite peaks are given by $\epsilon_{\uparrow}^{(n)} = \epsilon_0 + E_Z/2 \pm n\omega$ and $\epsilon_{\downarrow}^{(n)} = \epsilon_0 - E_Z/2 \pm n\omega$, with $n = 1, 2, 3, \dots$. For increasing ω , the satellite peaks tend to vanish and the system recovers its original two levels ϵ_{\uparrow}^0 and ϵ_{\downarrow}^0 . The horizontal dashed lines delimit the conduction window $[\mu_R, \mu_L]$. Units: Energy in units of Γ_0 and $\omega_0 = \Gamma_0/\hbar$.

Substituting this result into Eq. (6), the current can be written in its Landauer form⁴¹

$$\langle I_{\sigma}^L(t) \rangle = e \int \frac{d\epsilon}{2\pi} T_{\sigma}(\epsilon) [f_L(\epsilon) - f_R(\epsilon)]. \quad (8)$$

Here we define

$$T_{\sigma}(\epsilon) = \Gamma_{\sigma}^L \Gamma_{\sigma}^R \sum_{n=-\infty}^{\infty} \frac{J_n^2(\frac{\Delta}{\omega})}{(\epsilon - \epsilon_{\sigma}^{(n)})^2 + (\frac{\Gamma_{\sigma}}{2})^2}, \quad (9)$$

where $\epsilon_{\sigma}^{(n)} = \epsilon_{\sigma}^0 + n\omega$. Eq. (9) shows that the harmonic modulation of the dot level yields to photon-assisted peaks in the transmission coefficient.⁸ In addition to this, here we have the spin splitting of these peaks and the ferromagnetic leads, that results in an enhanced spin photon-assisted transport.

A further simplification can be made in Eq. (8) by considering the low temperature regime, where the Fermi functions are approximated by step functions. In this regime, the integral in Eq. (8) is carried out in the range $[\mu_L, \mu_R]$, thus resulting in

$$\langle I_{\sigma}^L \rangle = I_{\sigma}^0 \Phi_{\sigma}, \quad (10)$$

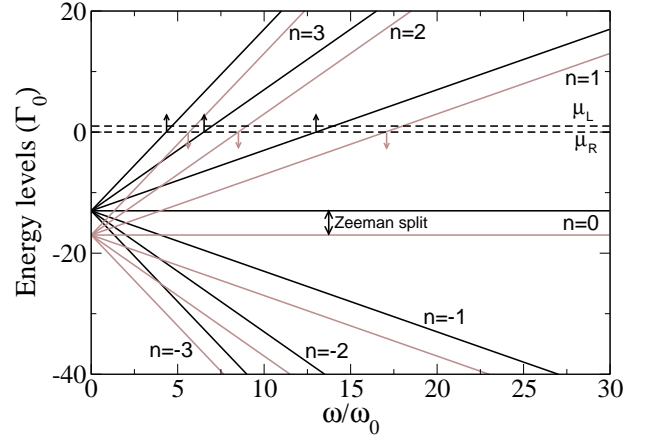


FIG. 3. Multiplet structure developed in the presence of an oscillating gate frequency. The black lines correspond to spin up while the gray lines to spin down. The levels are shifted linearly with the gate frequency, following $\epsilon_{\sigma}^{(n)} = \epsilon_{\sigma}^0 \pm n\omega$, $n = 1, 2, 3, \dots$. The up and down levels are Zeeman split. The horizontal dashed lines correspond to the left (μ_L) and to the right (μ_R) chemical potentials. The channels $\epsilon_{\uparrow}^{(n)}$ and $\epsilon_{\downarrow}^{(n)}$ attain resonance within the conduction window $[\mu_L, \mu_R]$ for certain frequencies, which differ for each spin component. Units: Energy levels in units of Γ_0 and $\omega_0 = \Gamma_0/\hbar$.

where $I_{\sigma}^0 = e \frac{\Gamma_{\sigma}^L \Gamma_{\sigma}^R}{\Gamma_{\sigma}^L + \Gamma_{\sigma}^R}$ is the resonant current without modulated gate voltage and

$$\Phi_{\sigma} = \sum_{n=-\infty}^{\infty} J_n^2\left(\frac{\Delta}{\omega}\right) [\Theta_n^{\sigma L}(\omega) - \Theta_n^{\sigma R}(\omega)] / \pi, \quad (11)$$

with $\Theta_n^{\sigma \eta}(\omega) = \arctan[2(\mu_{\eta} - \epsilon_{\sigma}^0 - n\omega)/\Gamma_{\sigma}]$. In what follows we present our numerical results to the spin polarized transport.

III. NUMERICAL RESULTS

Figure 2 shows the sum $T = T_{\uparrow} + T_{\downarrow}$ as a function of ω and energy in the case of polarized leads with parallel magnetizations. As ω increases, a multiplet structure takes place in the transmission coefficient [Eq. (9)]. The two central peaks in $T(\epsilon, \omega)$ correspond to ϵ_{\uparrow}^0 and ϵ_{\downarrow}^0 , while the lateral peaks are related to $\epsilon_{\sigma}^0 \pm n\omega$. Due to the Zeeman splitting, the whole pattern for T_{\uparrow} is shifted upward while T_{\downarrow} is moved downward. The highest of the peaks are strongly affected by the frequency. For the n -th peak its amplitude is given by $4\Gamma_{\sigma}^L \Gamma_{\sigma}^R J_n^2(\Delta/\omega)/\Gamma_{\sigma}^2$. For sufficiently large ω , the additional photon-assisted peaks are suppressed, remaining only the two central peaks. The broadening difference for up and down spin channels comes from the ferromagnetism of the electrodes that are parallel aligned, with majority down population in both sides ($p_L = p_R = -0.4$).

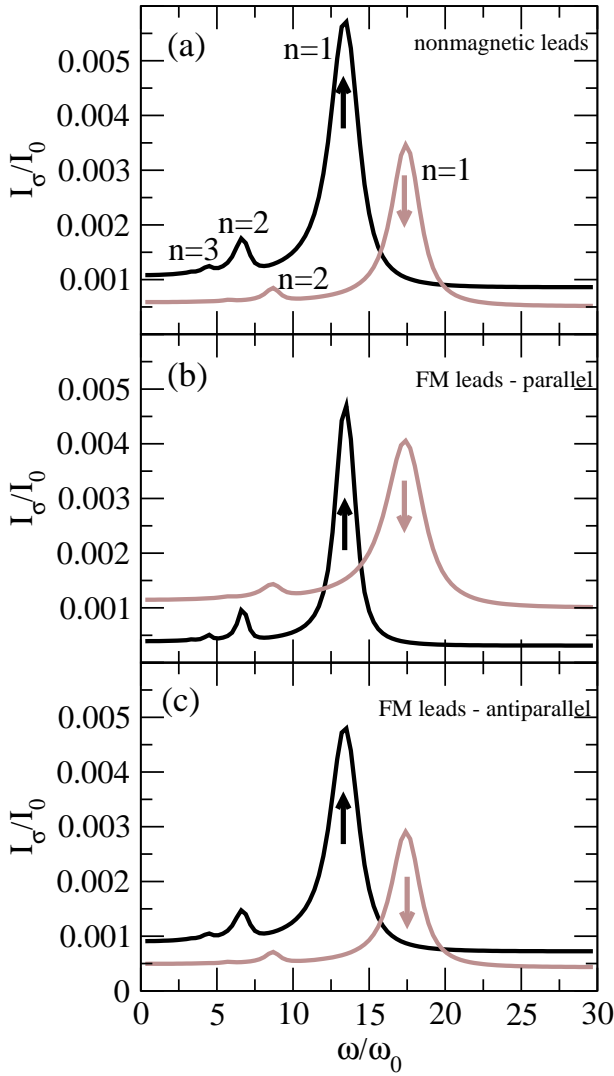


FIG. 4. Spin resolved currents against gate frequency for leads (a) nonmagnetic and (b)-(c) ferromagnetic. In panels (b) and (c) we show the parallel and antiparallel alignments, respectively. Both up and down currents show peaks corresponding to the crossing of $\epsilon_\uparrow^{(n)}$ and $\epsilon_\downarrow^{(n)}$ illustrated in Fig. (3). The highest peak for each spin component comes from the resonance of the levels $\epsilon_\uparrow^{(1)}$ and $\epsilon_\downarrow^{(1)}$, within the conduction window. In the parallel alignment the majority down population in both leads turns into an amplification of the down current. In the antiparallel case, though, the currents are very similar to the nonmagnetic case. Units: $I_0 = e\Gamma_0/\hbar$ and $\omega_0 = \Gamma_0/\hbar$.

Spin polarized transport can arise depending upon the position of the peaks of $T_\sigma(\epsilon, \omega)$ with respect to the conduction window. Fig. (3) shows the channels $\epsilon_\uparrow^0 + n\omega$ and $\epsilon_\downarrow^0 + n\omega$ for $n = 0, \pm 1, \pm 2, \pm 3$ as black and gray lines, respectively. The left and right chemical potentials are indicated by the horizontal dashed lines. A net electron transport from the left to the right lead can take place whenever a channel $\epsilon_\sigma + n\omega$ attains the interval $[\mu_L, \mu_R]$.

Due to the Zeeman splitting, each spin component crosses μ_L or μ_R at different frequencies, thus resulting in a frequency selective spin transfer between the leads. In Fig. (3) we indicate by up and down arrows the corresponding crossing of the conduction windows for spins \uparrow and \downarrow , respectively. In the present study we focus on the off-resonant regime, where the dot levels ϵ_\uparrow^0 and ϵ_\downarrow^0 are far below the conduction window. In this case only photon-assisted electrons can tunnel through the system. In order to match this condition we adopt to the numerical parameters the following values: $\epsilon_d^0 = -15\Gamma_0$, $E_Z = 4\Gamma_0$, $\Delta = 5\Gamma_0$, $\mu_L = 1\Gamma_0$ and $\mu_R = 0$. In experiments we find typically $\Gamma_0 \sim 100\mu\text{eV}$.⁴²⁻⁴⁴ So to the parameters assumed we have $E_Z \sim 400\mu\text{eV}$. This Zeeman energy split is reasonable for semiconductor quantum dots in the presence of magnetic fields $\sim 1-10$ T.⁴⁵ Additionally, for these values we find $\omega_0 = \frac{\Gamma_0}{\hbar} \sim 150$ GHz. So the present theoretical effects could be observed for gate frequencies around 1.5 THz [$\omega \sim 10\omega_0$, see Fig. (4)].⁴⁶ Alternatively, if Γ_0 is reduced to $\sim 1\mu\text{eV}$,^{47,48} we obtain gate frequencies around $\omega \sim 10\omega_0 \sim 15$ GHz, which is quite feasible experimentally.⁴⁹

Comparing Fig. (3) to Fig. (2) one can note that even though $n = 3$ and $n = 2$ attains resonance withing $[\mu_L, \mu_R]$, their corresponding transmission amplitude are very low, which makes the transport weak via those channels. In contrast, the $n = 1$ channels, for up and down spins, have a higher transmission amplitude, which makes the spin transfer via these channels more appreciable.

Fig. (4) shows the up and down components of the current against gate frequency. Three cases are considered: (a) nonmagnetic leads, ferromagnetic leads in the (b) parallel and (c) antiparallel alignments. In all the three cases two major peaks are found ($n = 1$). Satellite peaks for high order channels ($n = 2, 3$) are also seen. Each peak emerges whenever a channel $\epsilon_\sigma^0 + n\omega$ enters the conduction window [indicated by \uparrow and \downarrow arrows in Fig. (3)]. Due to the Zeeman splitting, the resonance for spin up arises in lower frequencies than that for spin down. Additionally, the interplay between Zeeman splitting and the amplitude of the transmission coefficient results into a higher peak for spin up than for spin down in the case of nonmagnetic leads.⁵⁰ Further amplification of the spin down current peak is observed when the leads are made ferromagnetic. In Fig. 4(b) we present I_\uparrow and I_\downarrow for leads parallel aligned, with a majority down population in both sides. This means that we assume for the polarization parameter a negative value, with $p_L = p_R = p = -0.4$. This implies that $\Gamma_\downarrow^{L,R} > \Gamma_\uparrow^{L,R}$ ($\rho_\downarrow^{L,R} > \rho_\uparrow^{L,R}$), which favors more the spin down electrons to tunnel through the system, thus increasing the spin down current peak. In the antiparallel case, where we have a majority down population in the left lead and a majority up population in the right lead ($\Gamma_\downarrow^L > \Gamma_\uparrow^L$ and $\Gamma_\downarrow^R < \Gamma_\uparrow^R$ for $p_L = -p_R = p = -0.4$), the incoming and outgoing rates compensate each other. This turns into equal weights for both up and down cur-

rents, so the current remains almost the same compared to the nonmagnetic case.

Fig. (5) shows how the spin resolved currents evolve when the leads polarizations are enlarged in both P and AP configurations. When p becomes more negative, the spin down tunneling rates Γ_{\downarrow}^L and Γ_{\downarrow}^R are strengthened, while Γ_{\uparrow}^L and Γ_{\uparrow}^R are diminished in the parallel case. This amplifies the peak for spin down current while suppresses the peak for spin up, thus making the current more down polarized. Eventually, for larger enough $|p|$ the I_{\downarrow} current dominates over I_{\uparrow} for all gate frequencies. Conversely, in the antiparallel configuration, as p turns more negative, both I_{\uparrow} and I_{\downarrow} are suppressed. One may note that when we pass from P to AP configuration, the major spin up peak has its width broadened. This can also be seen by calculating the width of this peak. For both P and AP we find $\Gamma_{\uparrow} = \Gamma_{\uparrow}^L + \Gamma_{\uparrow}^R = 2\Gamma_0(1 - |p|)$ and $\Gamma_{\downarrow} = \Gamma_{\downarrow}^L + \Gamma_{\downarrow}^R = 2\Gamma_0$ for P and AP configurations, respectively. Interestingly, this broadening effect makes the total antiparallel current slightly higher than the parallel current ($I^P < I^{AP}$), as we will see next.

Finally, in Fig. (6) we show the total current in both P and AP alignment and the tunnel magnetoresistance, defined according to

$$TMR = \frac{I^P - I^{AP}}{I^{AP}}, \quad (12)$$

where $I^{P/AP} = I_{\uparrow}^{P/AP} + I_{\downarrow}^{P/AP}$. The highest current peak is related to the resonance of the channel $\epsilon_{\uparrow}^{(1)} + \omega$ with the conduction window. The second highest peak is due to spin down resonance, $\epsilon_{\downarrow}^{(1)} + \omega \approx \mu_R$. The spin valve effect is clearly seen for almost all frequencies, i.e., $I^P > I^{AP}$. However, for frequencies around $10\omega_0$, we observe $I^P < I^{AP}$ for $p = -0.4$ [Fig. 6(a)]. This photon-assisted opposite spin valve effect is related to the broadening of the spin up peak discussed in Fig. (5), when the lead polarizations rotate from P to AP alignment. This feature is reflected in the TMR, which acquires negative values. Notice that near the position of the spin up peak the TMR is fully suppressed, while near to the peak of the spin down current it is enlarged for all values of p . This indicates that the magnetoresistance is mainly dominated by spin down transport.

IV. CONCLUSION

We have studied spin polarized transport in a quantum dot attached to ferromagnetic leads in the presence of an oscillating gate voltage $V_g(t)$. A static source-drain bias voltage is also applied in order to generate current. The oscillating $V_g(t)$ gives rise to photon-assisted transport channels that allow electrons to flow through the system. Due to a Zeeman splitting of the dot level, the photon-assisted contributions to the transport are distinct for spins up and down, providing an interesting way to obtain current polarization that can be controlled by gate

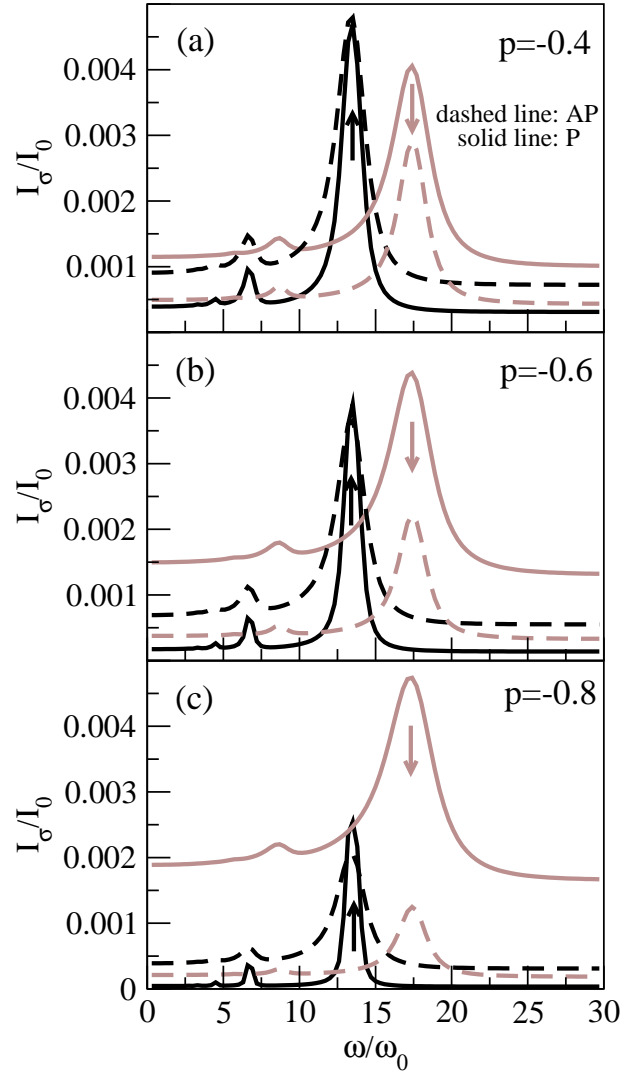


FIG. 5. Spin resolved currents against gate frequency for differing polarization degree p , in both parallel and antiparallel configurations. In the plots p is negative, which means that both leads have majority spin down population in the P case and majority down (up) population in the left (right) lead for the AP case. In the P alignment when p increases (in modulus) the tunneling rates between the dot and the leads enlarge for spin down and reduce for spin up. This results in an amplification of I_{\downarrow} and a suppression of I_{\uparrow} as observed. In the AP alignment both I_{\uparrow} and I_{\downarrow} are suppressed as $|p|$ increases. Units: $I_0 = e\Gamma_0/\hbar$ and $\omega_0 = \Gamma_0/\hbar$.

frequency. As the leads polarization is enlarged, with a majority down population in both leads (P alignment), the spin down photon-assisted current peak is enhanced, while the spin up peak is suppressed. Moreover, when the relative polarization alignment of the leads is switched from P to AP, the width of the main spin up peak of the current is broadened. This additional broadening effect results in an opposite spin valve behavior ($I^P < I^{AP}$) for gate frequencies around the spin up resonance. As

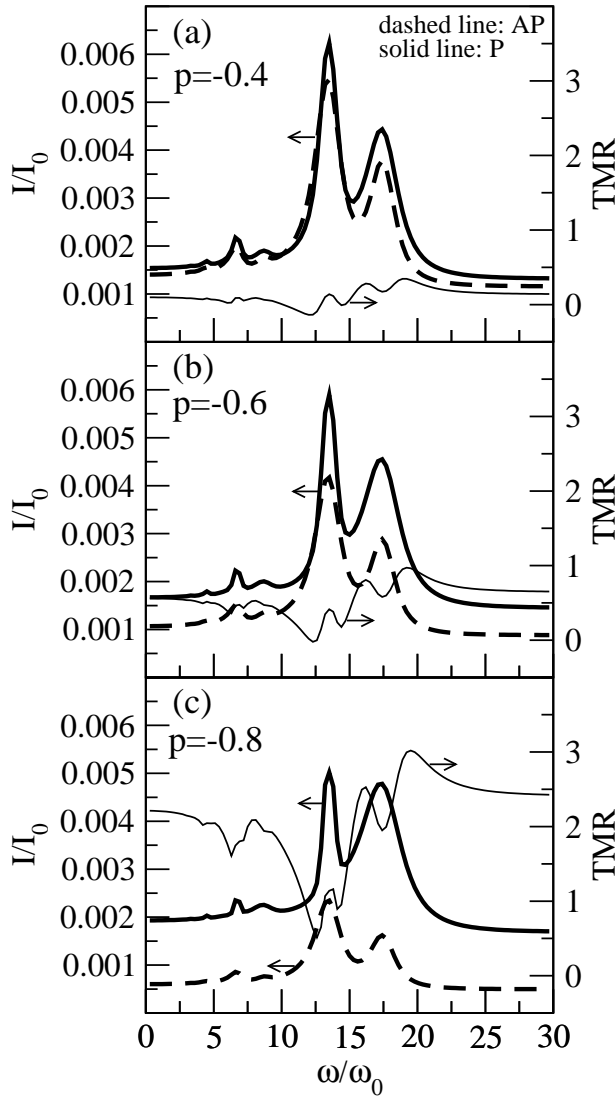


FIG. 6. Total current ($I_{\uparrow} + I_{\downarrow}$) in both P and AP alignment and TMR as a function of the gate frequency. From panels (a) to (c) the left and right leads polarization are enlarged ($p = -0.4, -0.6, -0.8$). The highest current peak is predominantly due to spin up transport while the second highest peak is more spin down like. The TMR tends to be suppressed or amplified around the spin up or spin down peaks, respectively. In particular, the TMR attains negative values for $p = -0.4$ in a short gate frequency range, due to a photon-assisted inversion of the spin valve effect ($I^P < I^{AP}$). Units: $I_0 = e\Gamma_0/\hbar$ and $\omega_0 = \Gamma_0/\hbar$.

a result, a photon-assisted negative tunnel magnetoresistance is found.

ACKNOWLEDGMENTS

The authors acknowledge A. P. Jauho and J. M. Villas-Bôas for valuable comments and suggestions. This work was supported by the Brazilian agencies CNPq, CAPES and FAPEMIG.

-
- ¹ N. S. Wingreen, A. P. Jauho, and Y. Meir, Phys. Rev. B **48**, 8487 (1993).
² L. J. Geerligs, V. F. Anderegg, P. A. M. Holweg, J. E. Mooij, H. Pothier, D. Esteve, C. Urbina, M. H. Devoret, Phys. Rev. Lett. **64**, 2691 (1990).
³ L. P. Kouwenhoven, A. T. Johnson, N. C. van der Vaart, C. J. P. M. Harmans, C. T. Foxon, Phys. Rev. Lett. **67**,

- 1626 (1991).
⁴ C. Bruder and H. Schoeller, Phys. Rev. Lett. **72**, 1076 (1994).
⁵ L. P. Kouwenhoven, S. Jauhar, K. McCormick, D. Dixon, P. L. McEuen, Yu. V. Nazarov, N. C. van der Vaart, and C. T. Foxon, Phys. Rev. B **50**, 2019(R) (1994).

- ⁶ L. P. Kouwenhoven, S. Jauhar, J. Orenstein, P. L. McEuen, Y. Nagamune, J. Motohisa, and H. Sakaki, *Phys. Rev. Lett.* **73**, 3443 (1994).
- ⁷ B. J. Keay, S. J. Allen, Jr., J. Galán, J. P. Kaminski, K. L. Campman, A. C. Gossard, U. Bhattacharya, and M. J. W. Rodwell, *Phys. Rev. Lett.* **75**, 4098 (1995).
- ⁸ For a review see G. Platero and R. Aguado, *Phys. Rep.* **395**, 1 (2004).
- ⁹ C. A. Stafford and N. S. Wingreen, *Phys. Rev. Lett.* **76**, 1916 (1996).
- ¹⁰ A. F. Amin, G. Q. Li, A. H. Phillips, and U. Kleinekathöfer, *Eur. Phys. J. B* **68**, 103 (2009).
- ¹¹ F. Cavaliere, M. Governale, and J. König, *Phys. Rev. Lett.* **103**, 136801 (2009).
- ¹² R. Zhu and H. Chen, *Appl. Phys. Lett.* **95**, 122111 (2009).
- ¹³ E. Prada, P. San-Jose, and H. Schomerus, *Phys. Rev. B* **80**, 245414 (2009).
- ¹⁴ G. M. M. Wakker and M. Blaauboer, *Phys. Rev. B* **82**, 205432 (2010).
- ¹⁵ M. Alos-Palop and M. Blaauboer, arXiv: 1102.0926 (2011).
- ¹⁶ J. Splettstoesser, M. Governale, J. König, and M. Büttiker, *Phys. Rev. B* **81**, 165318 (2010).
- ¹⁷ N. A. Lima, M. F. Silva, L. N. Oliveira, and K. Capelle, *Phys. Rev. Lett.* **90**, 146402 (2003).
- ¹⁸ S. Kurth, G. Stefanucci, E. Khosravi, C. Verdozzi, and E. K. U. Gross, *Phys. Rev. Lett.* **104**, 236801 (2010).
- ¹⁹ G. A. Prinz, *Science* **282**, 1660 (1998); S. A. Wolf, D. D. Awschalom, R. A. Buhrman, J. M. Daughton, S. von Molnár, M. L. Roukes, A. Y. Chtchelkanova, and D. M. Treger, *ibid.* **294**, 1488 (2001); *Semiconductor Spintronics and Quantum Computation*, edited by D. Awschalom, D. Loss, and N. Samarth (Springer, Berlin 2002); D. D. Awschalom and M. E. Flatté, *Nat. Phys.* **3**, 153 (2007).
- ²⁰ E. Cota, R. Aguado, and G. Platero, *Phys. Rev. Lett.* **94**, 107202 (2005).
- ²¹ R. Sánchez, E. Cota, R. Aguado, and G. Platero, *Phys. Rev. B* **74**, 035326 (2006); R. Sánchez, E. Cota, R. Aguado, and G. Platero, *Physica E* **34**, 405 (2006).
- ²² E. R. Mucciolo, C. Chamon, and C. M. Marcus, *Phys. Rev. Lett.* **89**, 146802 (2002).
- ²³ T. Aono, *Phys. Rev. B* **67**, 155303 (2003).
- ²⁴ S. K. Watson, R. M. Potok, C. M. Marcus, and V. Umansky, *Phys. Rev. Lett.* **91**, 258301 (2003).
- ²⁵ F. M. Souza, *Phys. Rev. B* **76**, 205315 (2007).
- ²⁶ E. Perfetto, G. Stefanucci, and M. Cini, *Phys. Rev. B* **78**, 155301 (2008).
- ²⁷ P. Trocha, *Phys. Rev. B* **82**, 115320 (2010).
- ²⁸ F. M. Souza, S. A. Leão, R. M. Gester, and A. P. Jauho, *Phys. Rev. B* **76**, 125318 (2007).
- ²⁹ F. M. Souza and J. A. Gomez, *Phys. Status Solid B* **246**, 431 (2009).
- ³⁰ R. Hanson and D. D. Awschalom, *Nature* **453**, 1043 (2008).
- ³¹ J. M. Elzerman, R. Hanson, L. H. W. van Beveren, B. Witkamp, L. M. K. Vandersypen, and L. P. Kouwenhoven, *Nature* **430**, 431 (2004).
- ³² R. Hanson, L. H. W. van Beveren, I. T. Vink, J. M. Elzerman, W. J. M. Naber, F. H. L. Koppens, L. P. Kouwenhoven, and L. M. K. Vandersypen, *Phys. Rev. Lett.* **94**, 196802 (2005).
- ³³ A. C. Johnson, J. R. Petta, J. M. Taylor, A. Yacoby, M. D. Lukin, C. M. Marcus, M. P. Hanson, and A. C. Gossard, *Nature* **435**, 925 (2005).
- ³⁴ J. R. Petta, A. C. Johnson, J. M. Taylor, E. A. Laird, A. Yacoby, M. D. Lukin, C. M. Marcus, M. P. Hanson, A. C. Gossard, *Science* **309**, 2180 (2005).
- ³⁵ F. H. L. Koppens, C. Buizert, K. J. Tielrooij, I. T. Vink, K. C. Nowack, T. Meunier, L. P. Kouwenhoven, and L. M. K. Vandersypen, *Nature* **442**, 766 (2006).
- ³⁶ C. Barthel, J. Medford, C. M. Marcus, M. P. Hanson, and A. C. Gossard, *Phys. Rev. Lett.* **105**, 266808 (2010).
- ³⁷ H. Haug and A. P. Jauho, *Quantum Kinetics in Transport and Optics of Semiconductors*, Springer Solid-State Sciences **123** (1996).
- ³⁸ In the present calculation we follow the formulation developed in A. P. Jauho, N. S. Wingreen, and Y. Meir, *Phys. Rev. B* **50**, 5528 (1994).
- ³⁹ W. Rudziński and J. Barnaś, *Phys. Rev. B* **64**, 85318 (2001).
- ⁴⁰ F. M. Souza, J. C. Egues, and A. P. Jauho, *Braz. J. Phys.* **34**, 565 (2004).
- ⁴¹ An alternative but equivalent version of this equation was derived in Ref. [8], where the distinction between this result and the Tien-Gordon formula was discussed.
- ⁴² D. G.-Gordon, H. Shtrikman, D. Mahalu, D. A.-Magder, U. Meirav, M. A. Kastner, *Nature* **391**, 156 (1998).
- ⁴³ D. Goldhaber-Gordon, J. Göres, M. A. Kastner, H. Shtrikman, D. Mahalu, and U. Meirav, *Phys. Rev. Lett.* **81**, 5225 (1998).
- ⁴⁴ F. Simmel, R. H. Blick, J. P. Kotthaus, W. Wegscheider, and M. Bichler, *Phys. Rev. Lett.* **83**, 804 (1999).
- ⁴⁵ R. Hanson, B. Witkamp, L. M. K. Vandersypen, L. H. Willems van Beveren, J. M. Elzerman, and L. P. Kouwenhoven, *Phys. Rev. Lett.* **91**, 196802 (2003).
- ⁴⁶ Significant improvements on THz electronics have been recently achieved. See for instance, T. W. Crowe, W. L. Bishop, D. W. Porterfield, J. L. Hesler, R. M. Weikle, *IEEE J. Solid-State Circuits*, **40**, 2104 (2005).
- ⁴⁷ S. Amasha (private communication).
- ⁴⁸ K. MacLean, S. Amasha, I. P. Radu, D. M. Zumbühl, M. A. Kastner, M. P. Hanson, and A. C. Gossard, *Phys. Rev. Lett.* **98**, 036802 (2007).
- ⁴⁹ H. Eisele, S. P. Khanna, and E. H. Linfield, *Appl. Phys. Lett.* **96**, 072101 (2010).
- ⁵⁰ Two split peaks in a pumping current, one peak for each spin component, were also found by Cota et al. in Ref. [20] for a double dot system in the presence of magnetic field.